

First-Principles Studies of phonons in Na_xCoO_2 Yirigui,¹ G. J. Zhao,^{1,*} and X. X. Liang¹¹*Department of Physics, Inner Mongolia University, Hohhot 010021, PR China*

(Received April 9, 2010)

By using the density functional theory with GGA approach, we study the phonon dispersion of Na_xCoO_2 . Two Na atomic positions are considered in calculation. The phonon dispersion and the phonon density of state for Na concentration $x = 0.6$ are obtained and compared with experimental and other theoretical results.

PACS numbers: 63.20.dk, 63.20.kd, 74.25.kc

I. INTRODUCTION

The layered material Na_xCoO_2 ($0 < x < 1$) has become of interest in condensed matter studies in no small part due to the existence of thermoelectric property, Terasaki and co-workers [1] have discovered large thermoelectric power in this materials and proposed that the compound is of importance in view of potential application in thermoelectric devices which can carry out energy conversion from heat to electrical energy. Compared with traditional thermoelectric materials, Na_xCoO_2 is of higher applied temperature, oxidation resistant and longer service life. There is a great deal of experimental and theoretical research on the thermoelectric, electronic and phonon properties of this material system [2–4].

The efficiency of thermoelectric material is determined by a figure of merit $ZT = \sigma S^2 T / \kappa$, where σ is the electrical conductivity and S is the thermoelectric power, the quantity in the denominator is the thermal conductivity which is given by the sum of contributions from the electronic carries κ_e and the lattice κ_l . The efficiency is increased by making ZT as large as possible where T is the main operating temperature of the device. S, σ and κ_e are mainly related to the electronic structure, they can not change independently. So the main way [5] to improve the figure of merit is to reduce the lattice thermal conductivity through the enhancement of phonon scattering.

In this article, we have investigated the phonon dispersion relation of Na_xCoO_2 with first-principles calculation.

II. COMPUTATIONAL METHOD AND STRUCTURE MODEL

In this article the calculation of phonon dispersion relations of Na_xCoO_2 is done in the framework of the density functional theory. Exchange-correlation effect is treated in the framework of generalized approximation using a functional proposed by Perdew-

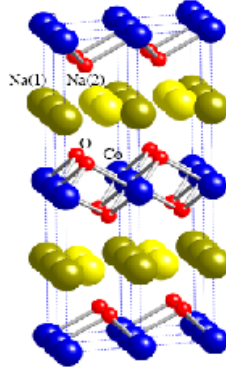


FIG. 1: The conventional unit cell of Na_xCoO_2 .

Burke-Ernzerhof [6] which is found to reproduce correctly result for a wide range of crystal structures. The wave functions are expanded in a plane-wave basis. The kinetic energy cutoff of the plane wave basis is 40 Hartree. Brillouin zone integration is performed using $2 \times 2 \times 2$ k point mesh. The real space forces constant is obtained through the Fourier Transformation of dynamical matrices. The whole calculation is carried out by the Quantum Espresso code [7]. The crystal structure parameters of Na_xCoO_2 used in my calculation can find in Ref. [8].

Hexagonal Na_xCoO_2 is a layered structural compound which has triangular CoO_2 layers with Na ions distributed in the intervening layers. There are two types of Na sites in this structure denoted as Na(1) and Na(2), as shown in Fig. 1. The lattices constant of Na_xCoO_2 is $a = 2.8244 \text{ \AA}$, and $c = 11.0046 \text{ \AA}$, that is to say, the concentration of Na atom is $x = 0.6$, the atomic positions of Na_xCoO_2 are Co: $2a(0, 0, 0)$, Na (1): $2b(0, 0, 1/4)$, Na (2): $2d(2/3, 1/3, 1/4)$, and O: $4f(1/3, 2/3, 0.0887)$, respectively.

III. RESULT AND DISCUSSION

The phonon dispersion relation of $\text{Na}_{0.6}\text{CoO}_2$ for Na(1) and Na(2) are presented in Fig. 2. We can see some interesting features from above spectrum. Firstly, the phonon curves have been separated into two groups clearly with their frequencies both in the two case of Na atomic position, which is ranged from 0 to 420 cm^{-1} and 450 to 575 cm^{-1} for the Na(1). The phonon spectrum of Na(2), however, has a smaller gap between two groups which are ranged from 0 to 418 cm^{-1} and from 421 to 575 cm^{-1} . We can see that the site of Na in the $\text{Na}_{0.6}\text{CoO}_2$ structure affect the phonon relations slightly from the above result. Secondly, the phonon curves in the range of 0 to 410 are obviously dispersive than the other one in both of Na(1) and Na(2). Thirdly, in the long-wave limit of the computed frequency of transverse and longitudinal acoustic branches (TA and LA) are almost linearly increased with wave vector around the Γ point.

The corresponding phonon density of state(DOS) is presented in Fig. 3. Because of

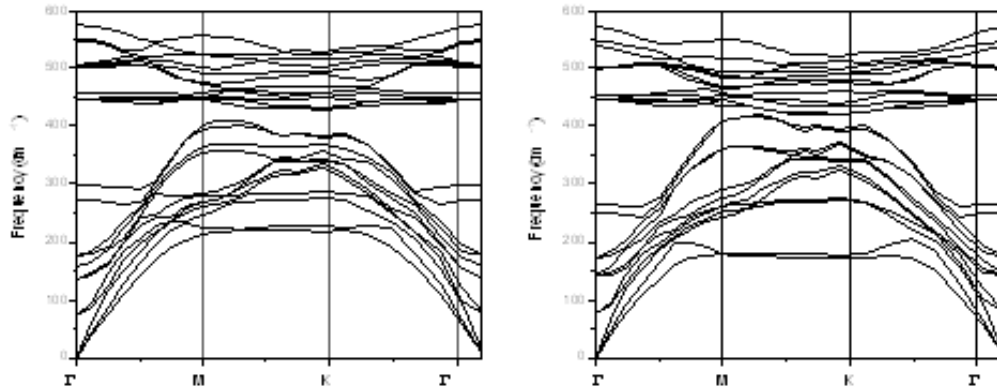


FIG. 2: Phonon dispersion curves of $\text{Na}_{0.6}\text{CoO}_2$ for Na(1) (left) and Na(2) (right).

the overlap of acoustic and optical phonon branches, there is no visible gap in the phonon DOS diagram between them. Relative to the flatness of phonon curves in the range of 430 to 600 cm^{-1} , there is a sharp peak at about 453 cm^{-1} for Na(1) and about 508 cm^{-1} for Na(2). Our calculated results of frequencies and phonon density of state are in good agreement with experimental and theoretical results of other workers, such as Ref. [2], in which Li *et al.* investigate the lattice vibrational properties of NaCoO_2 with ABINIT code [9].

In order to compare easily with the data, we list the results of calculated frequencies of the zone-center phonons in TABLE I.

For the Na_xCoO_2 structure, there are eight atoms with 24 degree of freedom per primitive unit cell. According to the group theoretical analysis [10], there are 3 acoustic modes and 15 optical modes at the Γ point of the Brillouin zone, which is consist of the

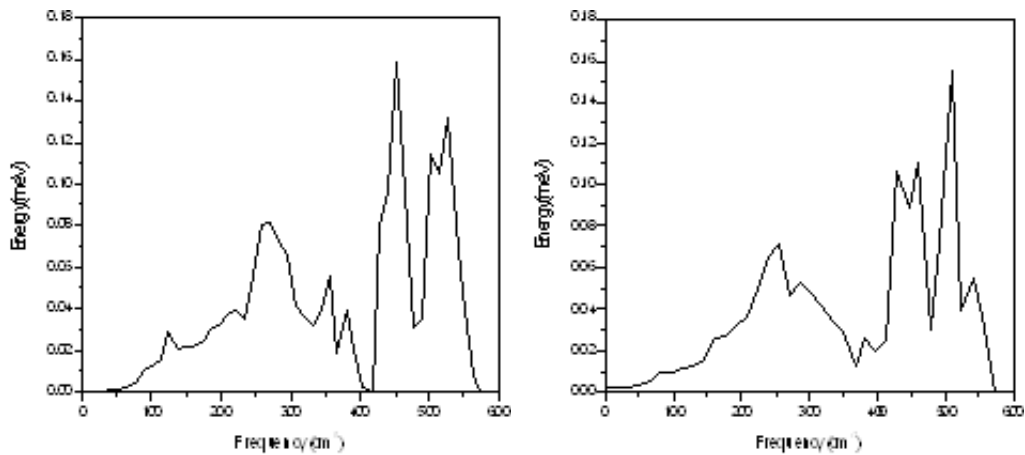


FIG. 3: Phonon density of state of $\text{Na}_{0.6}\text{CoO}_2$ for Na(1) (left) and Na(2) (right).

TABLE I: Zone center phonon modes of $\text{Na}_{0.6}\text{CoO}_2$ for Na(1)(left) and Na(2)(right).

symmetry	Phonon frequency(cm^{-1})	
	Na(1)	Na(2)
B_{1g}	73.3277	74.7770
E_{1u}	137.4915	141.4620
B_{2u}	155.5527	142.2158
A_{1g}	174.7905	173.0724
E_{2u}	275.0905	251.5447
A_{2u}	297.1746	264.1102
E_{2g}	445.1463	445.6024
E_{1g}	449.1586	447.2899
A_{2u}	459.1986	454.9129
B_{1g}	501.0894	499.7906
E_{1u}	504.7402	500.6821
E_{2g}	546.8712	538.2882
B_{2u}	550.1618	545.8501
E_{2u}	574.7180	571.7974

following irreducible representations of the point group D_{6h} :

$$\Gamma = (A_{1g} + E_{1g} + 3E_{2g}) + (2E_{1u} + 2A_{2u}) + (2E_{2u} + 2B_{2u} + B_{2g}).$$

The three acoustic phonon modes are triply-degenerated with zero frequency. The above 15 optical phonon modes, E_{2g} , E_{1g} and A_{1g} are Raman active, the infrared inactive E_1 and A_1 are infrared active and the remains are silent modes. For above five Raman active modes, E_{1g} mode is in-plane oxygen mode, A_{1g} mode is an out of-plane mode and E_{2g} modes are related to Na and oxygen. Raman active E_{1u} involve out-of-plane motions of Na, Co and oxygen atoms. The modes in the last bracket are both infrared inactive and Raman inactive namely silent modes.

TABLE II: Compared with Raman and infrared experimental results.

	Experimental Data (cm^{-1})	Our calculation results (cm^{-1})	
		Na(1)	Na(2)
Raman frequency of $\text{Na}_{0.7}\text{CoO}_2$ (Ref. [11])	A_{1g} (573)	504.7402	500.6821
	E_{1g} (458)	445.1463	445.6024
Raman frequency of $\text{Na}_{0.74}\text{CoO}_2$ (Ref. [12])	A_{1g} (586/576)	504.7402	500.6821
	E_{1g} (458/457)	445.1463	445.6024
Infrared frequency of (Ref. [13])	E_{1u} (570)	550.1618	545.8501

We have list the Raman and infrared experimental data in TABLE II and compare our calculated phonon frequencies with other results, through comparison we can see, our results

TABLE III: Phonon frequencies of high symmetry point M and K in Na(2).

	Phonon frequency(cm^{-1})			Phonon frequency(cm^{-1})	
	M point(0, 1/2, 0)	K point(-1/3, 2/3, 0)		M point(0, 1/2, 0)	K point(-1/3, 2/3, 0)
1	178.1421	173.4955	13	436.0700	422.3343
2	180.1000	178.6329	14	442.8549	423.8673
3	242.8388	269.5891	15	447.8896	434.4426
4	252.1960	274.7072	16	454.2928	442.1759
5	260.1979	311.0340	17	457.8049	459.3827
6	260.9570	318.8217	18	466.1678	472.8291
7	276.0749	343.1505	19	468.7048	482.2241
8	289.9897	348.6055	20	484.7206	487.1041
9	360.0205	351.6986	21	488.4304	493.9658
10	360.3788	358.1058	22	495.2969	502.7059
11	408.5036	396.9061	23	518.5697	507.7786
12	410.7833	401.7289	24	547.6825	525.6557

agree well with the experimental results. Li and Lemmens had done similar calculation with different method and calculation code in Ref. [2] and Ref. [12], respectively, our result are good agreement with theirs.

Because general trend of frequencies for Na(1) at high-symmetry point K and M are very similar with Na(2), we list the calculated frequencies at the remaining high-symmetry point K and M for Na(2) in the TABLE III. We can see that the frequencies for other high-symmetry point are all singly degenerated, distinctly differ from the case of Γ point, which has doubly and thirdly degenerated modes. We think that, the difference of the feature in degeneration between Γ point and other high symmetry points may be because that Γ point has higher symmetry than others.

IV. CONCLUSION

In this article, we study the phonon dispersion relation and density of state of Na_xCoO_2 for Na concentration $x = 0.6$. According to the results, for both cases we calculated, from the frequency point of view, the phonon spectrum can be divided into two parts, in the Na(1) case, the first part of the frequency range is from 0 to 410 cm^{-1} , the second part of the frequency range is from 430 to 575 cm^{-1} . While, in the Na(2) case, one part is from 0 to 418 and another part is from 421 to 572 cm^{-1} . The gap in Na(2) case is quite smaller than in Na(1) case. The optical phonon frequencies at M and K points are indicate singly degenerated characteristic unlike the center of Brillouin zone phonon modes. Finally, the acoustic phonon frequencies are almost linearly increased with wave vector around the Γ point.

Acknowledgments

This work was supported by the National Natural Science Foundation of China (Grant No. 10764003), the Natural Science Foundation of Inner Mongolia Autonomous Region of PR China (Grant No. 200711020105), the Educational Science Foundation of Inner Mongolia Autonomous Region of PR China (Grant NJ06048), and 531 Project of Inner Mongolia University.

References

- * Electronic address: stzhaogj@imu.edu.cn
- [1] I. Terasaki, Y. Sasago, and K. Uchinokura, *Phys. Rev. B* **56**, R12685 (1997).
 - [2] Z. Li, J. Yang, J. G. Hou, and Q. Zhu, *Phys. Rev. B* **70**, 144518 (2004).
 - [3] Q. Zhang, M. An, S. Yuan, Y. Wu, D. Wu, J. Luo, N. L. Wang, W. Bao, and Y. Wang, *Phys. Rev. B* **77**, 045110 (2008).
 - [4] B. J. Powell, J. Merino, and R. H. McKenzie, *Phys. Rev. B* **80**, 085113 (2009).
 - [5] G. Slack, in *CRC Handbook of Thermoelectrics*, Eds. D. M. Rowe (CRC, Boca Raton, Florida, 1995)p.407.
 - [6] J. P. Perdew, K. Burke, and M. Ernzerhof, *Phys. Rev. Lett.* **77**, 3685 (1996).
 - [7] P. Giannozzi, S. Baroni, N. Bonini and *et al.*, *J. Phys.: Condens. Matter* **21**, 395502(2009).
 - [8] Q. Huang, M. L. Foo, R. A. Pascal, Jr., J. W. Lynn, B. H. Toby, Tao He, H. W. Zandbergen, and R. J. Cava, *Phys. Rev. B* **70**, 184110(2004).
 - [9] X. Gonze, J. M. Beuken, R. Caracas and *et al.*, *Comput. Mater. Sci.* **25**, 478(2002).
 - [10] G. Y. Zhang, G. X. Lan and Y. F. Wang, *Lattice vibration spectroscopy*, 2nd ed. (High Educational Press, Beijing, 2006), Chap 6.
 - [11] M. N. Iliev, A. P. Litvinchuk, R. L. Meng, Y. Y. Sun, J. Cmaidalka and C. W. Chu, *Physica C* **402**, 239, (2004).
 - [12] P. Lemmens, V. Gnezdilov, N. N. Kovaleva, K. Y. Choi, H. Sakurai, E. Takayama-Muromachi, K. Takada, T. Sasaki, F. C. Chou, D. P. Chen, C. T. Lin and B. Keimer, *J. Phys.: Condens. Matter* **16**, S857 (2004).
 - [13] S. Lupi, M. Ortolani, and P. Calvani, *Phys. Rev. B* **69**, 180506(R)(2004).